Solid Freeform Fabrication Laser Tracking Control

Ying-Jeng Engin Wu and Joseph J. Beaman
Department of Mechanical Engineering
The University of Texas at Austin

Abstract

In order to increase productivity in Solid Freeform Fabrication (SFF) applications, a time-efficient laser tracking control technique is developed and simulated. An optimal solution of this minimum time control problem is obtained by a phase-plane technique. Due to the variable speed of time-efficient tracking, laser power intensity must be controlled in real time for uniform solidification. To achieve this requirement, an acousto-optic modulator is used. An experimental solidification model is used for laser power control.

I. Introduction

A time-efficient laser tracking control technique is desirable in SFF when one needs to trace the boundary of a part. Conventional raster scanning is not appropriate. A straight-line vector scanning mode can be slow when curves exist in the contour path due to repetitive starts and stops. A control must be achieved with a trade-off between rapid scanning speed, available scanning torque or force, uniform laser exposure, available laser power, and continuity of sintering. Besides this trade-off, a simple computer control algorithm is required since a very short sampling interval is needed due to the high tracking speed achieved by a scanning system used in SFF. Several articles have presented various schemes in this problem. The preview scheme (Tomizuka, Dornfeld, Bian, and Cal, 1984) [1] and the adaptive algorithm (Tsao, and Tomizuka, 1987)[4] need on-line computation effort which is too large for SFF application. The cross coupled compensator (Kulkarni and Srinivasan, 1985)[3] is designed to reduce the tracking error (minimizing the contour error) at a sharp corner, however contouring analysis and optimal speed trajectories are not developed for more general paths. The control trajectory scheme (Doraiswami, and Gulliver, 1984)[2] is directly obtained from a specified path with three simple functions regardless of the capability of actuator. The trajectory generation scheme (Butler, Haack and Tomizuka, 1988)[5] focuses on constant tracking speed which does not give a minimum time solution.

To solve the problem stated above, a minimum time optimal control problem is formulated and solved (Wu and Beaman, 1990)[8] . The control strategy used in this paper is based upon the results [8] of Pontryagin's minimum principle and phase plane techniques (Bobrow, Dubowsky and Gibson, 1985)[6], (Shin and McKay, 1985)[7].

The overall scanner control system is shown in fig.1, the laser beam is generated from a CO_2 laser, passes through an acousto-optic modulator which controls laser power, then, is focused by optics and reflected by a pair of mirrors driven by a pair of galvonometers, arrives at the working surface with a nonlinear geometric relation (e = 0.75", d = 12" in fig.1) between the mirror angle (controlled) and laser spot position on the working surface (specified). A sample test path is shown in fig.2. The following sections include modelling and identification of physical subsystems, minimum time control trajectory planning, feedback control design and simulation, conclusions and references.

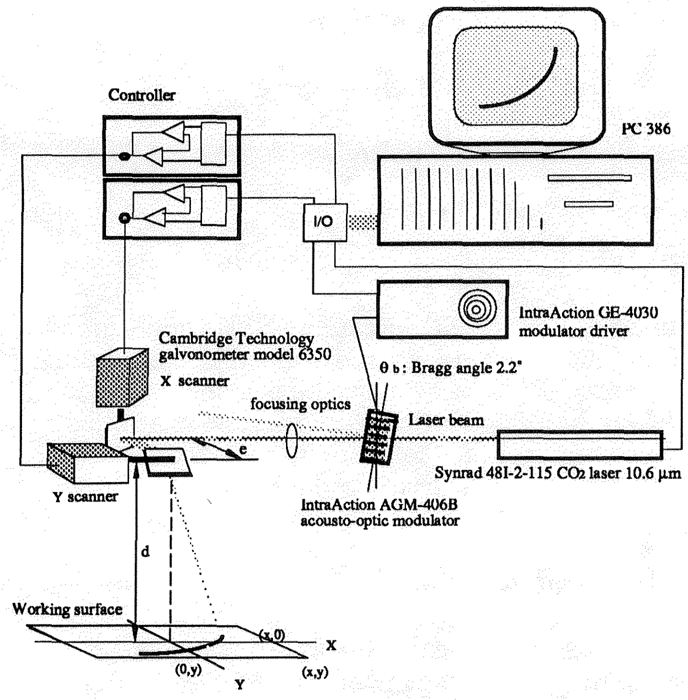

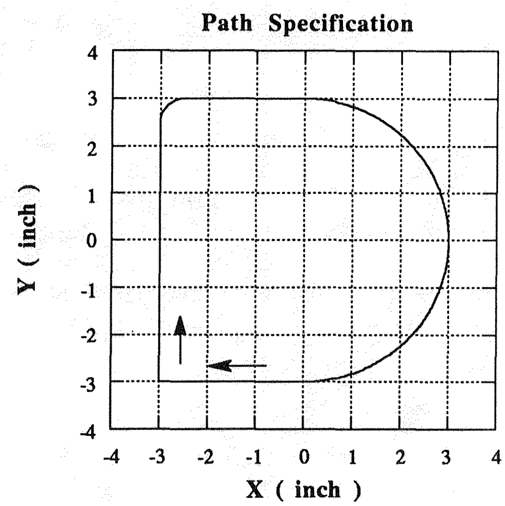

fig.1 The scanner control system

fig.2 The specified path

II. Modelling and identification of physical subsystems

Model of galvanometer : Galvonometers are basically D'Arsonval mechanisms. For this application, they should be designed with low inertia so the bandwidth is wide enough to be used as a servo-driver with low external load. Such a device with either moving coil or moving iron is called a galvanometer (Doebelin, 1975) [9], (Montagu, 1985) [10] widely used in laser scanning systems. Two moving coil galvanometer-mirror devices, model 6350 from Cambridge Technology Inc., are used. The galvonometer system diagram is shown in fig.3.

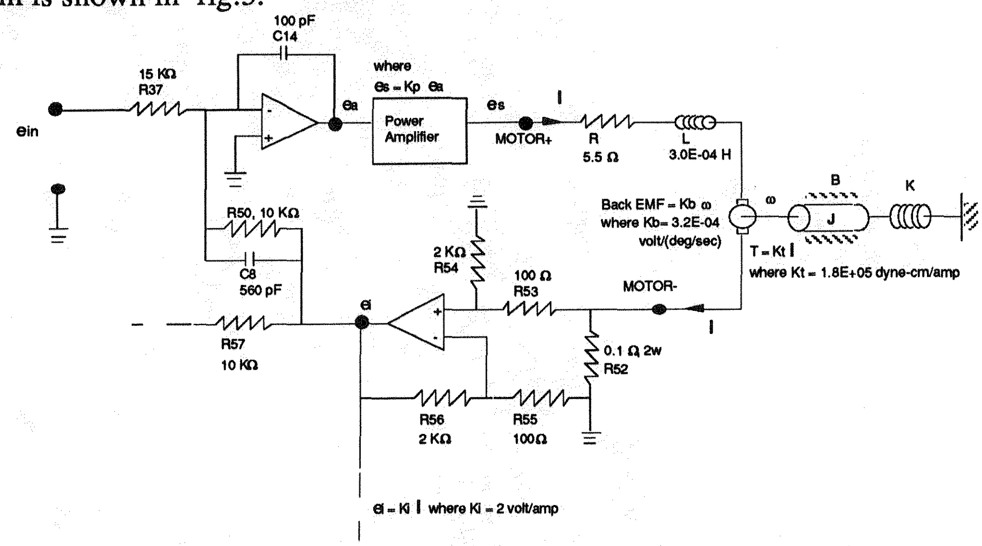

fig.3 System diagram of Galvanometer with Power amplifier
(model 6350, CB6500 Cambridge Technology, Inc.)[11]

After using both frequency domain and time domain techniques, the transfer function of a galvonometer system was identified as :

X axis : $$\frac{\theta(s)}{e_{in}(s)} = \frac{-4.2167e14}{s^4 + 3.0630e04s^3 + 2.2288e09s^2 + 3.1083e10s + 1.0905e13}$$

with two pairs of poles located at 1.1133e+01 Hz and 7.5134e+03 Hz, and

Y axis : $$\frac{\theta(s)}{e_{in}(s)} = \frac{-3.3573e13}{s^4 + 1.9917e04s^3 + 3.0227e08s^2 + 4.3247e09s + 7.2457e11}$$

with two pairs of poles located at 7.7957 Hz and 2.7658e+03 Hz.

Since one pair of poles is far away from the other, a simplified model of a galvonometer system may be used for the optimal control trajectory as

X axis :

$$\frac{\theta(s)}{e_{in}(s)} = \frac{-1.9225e05}{s^2 + 1.4102e01s + 4.9717e03}\ ; \text{ with } \xi = 0.1,\ \omega_n = 70.51 \text{ rad/sec} = 11.22 \text{ Hz;}$$

Y axis :

$$\frac{\theta(s)}{e_{in}(s)} = \frac{-1.1990e05}{s^2 + 1.5261e01s + 2.5878e03}\ ; \text{ with } \xi = 0.15, \omega_n = 50.87 \text{ rad/sec} = 8.10 \text{ Hz.}$$

The difference between the complete model and the simplified model is shown in fig.4.

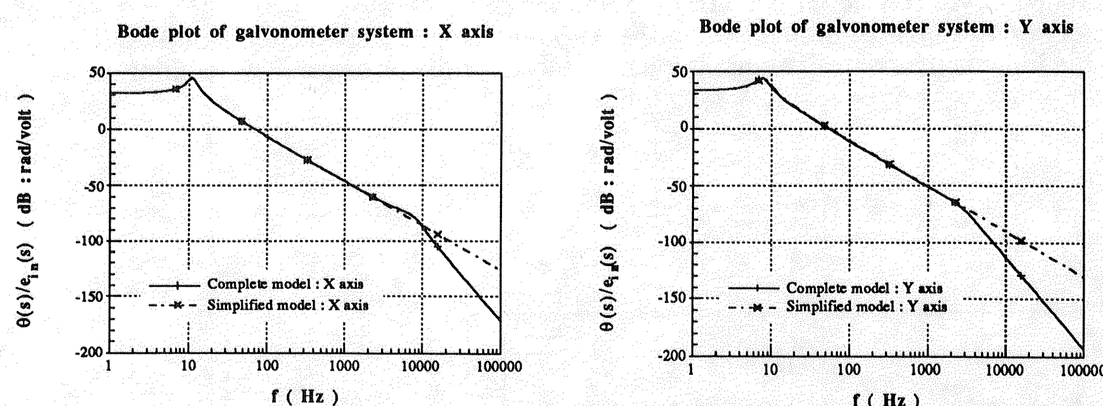

fig.4 Bode plot of complete/simplified galvonometer model

Laser power on-line control : For uniform solidification in SFF applications, laser power intensity must be controlled in real time. To achieve this requirement, the laser beam power must have good time stability and laser beam power modulation must be used.

(1) Laser beam power : The CO_2 laser, 10.6 μm wave length, is chosen in this project due to the good absorption by almost any spectrum of polymer materials. A water-cooled Synrad 48I-2-115 CO_2 laser is used. After 30-minute warm-up, its power variation is less than ±2% with 1.2 Gal/min cooling water flow at the room temperature. The measurement result is shown in fig.5.

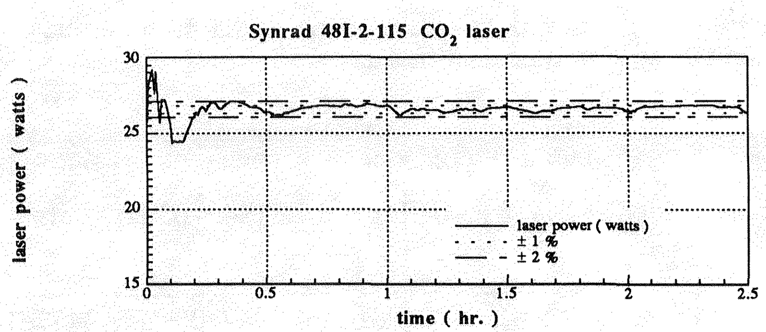

fig.5 Stability measurement of the laser power source

(2) Laser beam modulator : There are two types of laser beam modulators, electro-optic and acousto-optic. A linear electro-optic effect implies that change of refraction index is proportional to a controlled electrical field applied on certain crystals. Laser beam intensity modulator is constructed by use of an electro-optic crystal, a pair of optical crossed polarizers and a modulation signal source. (Amnon Yariv, 1985)[12], (Robert Goldstein, 1986)[13] An acousto-optic effect occurs when an acoustic wave travels through certain materials, that produces a sinusoidal stain field. A change of of refraction index is caused by the induced change in the density of material. The incident laser beam can then be refracted. The deflection angle of the refracted beam is controlled by the acoustic frequency of driving signal. The intensity of the refracted beam is controlled by the amplitude of driving signal. (Amnon Yariv, 1985)[12], (Adrian Korpel, 1988)[14], (J. Sapriel, 1979)[15], (Robert Adler, 1967)[16], (John Lekavich, 1986)[17].

In this paper, an IntraAction AGM-406B infrared acousto-optic modulator (Crystal Germanium) and GE-4030 light modulator driver are used to control the intensity of laser beam. Its bandwidth is about 0.7 MHz. (IntraAction Corp. 1990)[18] The input-output characteristic must be calibrated, where the output is the power percentage of output beam I_0 and the input is the controlled input voltage of the modulator driver. The calibration setup is shown in fig.6, and the result is shown in fig.7.

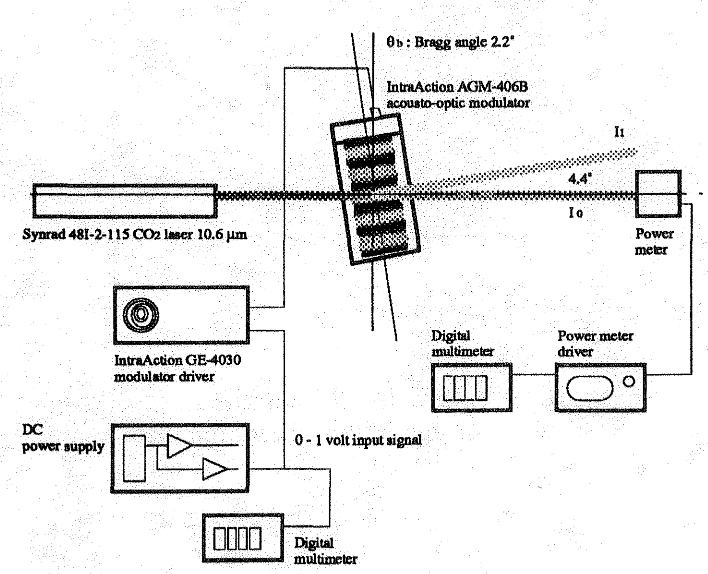

fig.6 Calibration setup

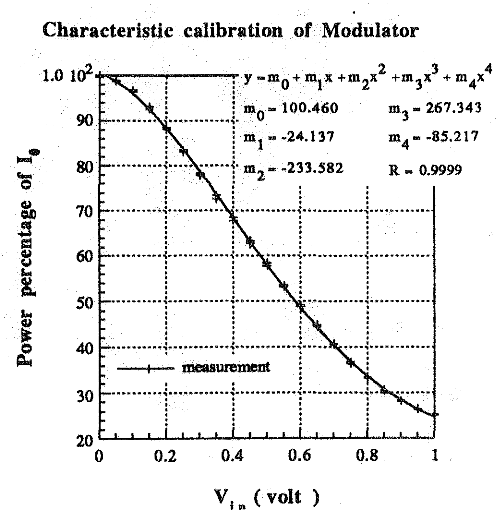

fig.7

Experimental model of solidification : Since a detailed mathematical model of solidification is difficult and complicated, the following experimental procedures are used to obtain a rough relation between the degree of solidification (its depth is used here), and laser power and scanning speed.(1) Measure the sintering depth (ds) with varying laser power (P). (2) Measure the sintering depth with varying scanning speed (V). (3) Make a plot with ds vs. P & 1/V. (shown in fig.8) Rough results show that ds $\propto$ P and ds $\propto$ 1/V.

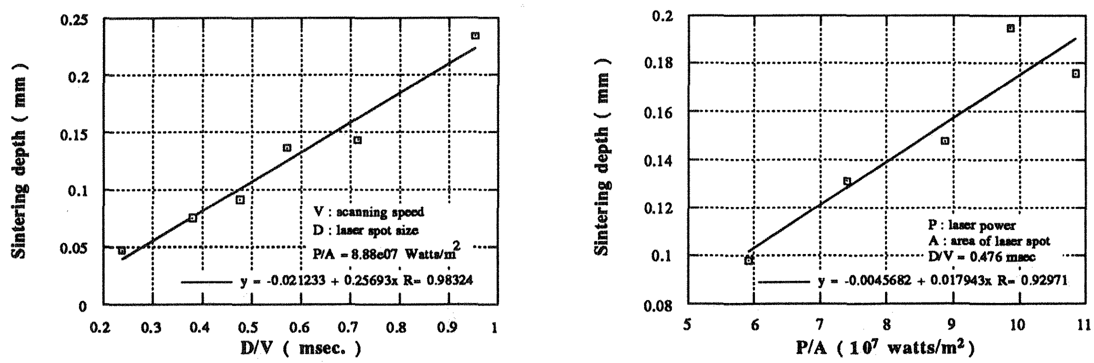

fig.8 Relation between the degree of solidification and laser power and scanning speed

III. Control trajectory planning

Based on the galvonometer model identified in section II, the minimum time optimal control is formulated with the specified path shown in fig.2. Pontryagin's minimum principle shows that no singular subarc exists [8], the solution is always on one boundary of the control inequality constraints. The solution is then obtained on a phase plane. The optimal trajectory is shown in fig.9.

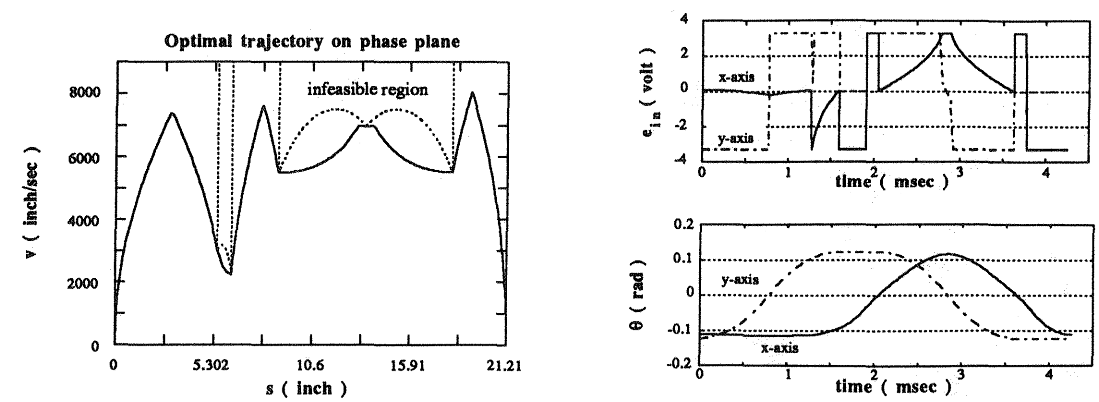

fig.9 The optimal trajectory

Fig.9 demonstrates optimal tracking speed on the order of thousands of inches per second, without the constraint of limited laser power. If unlimited laser power is assumed and the effect of air drag force on the moving mirror is ignored, the optimal trajectory may be achieved only when the conditions shown below are satisfied : (1) An extremely wideband (at least 50K Hz) power amplifier is used for the galvonometer. (2) An extremely short sampling interval (less than 5 microsecond) is required for the digital controller. (3) A fast data acquisition board (200K Hz for each channel) is required.

However, the allowable tracking speed may decrease when the effect of air drag force is added into the model and a larger mirror required for the high power laser increases the external load. The laser used in this paper is 25 watts. From lab data, approximately 50 inch/sec. is used for polymer sintering and 320 inch/sec. may leave a trace on a piece of color-coated paper under 25 watts. Therefore, tracking speed is limited to 320 inch/sec. (shown in fig.10) and is used for the rest of this paper. Note that tracking speed is accelerated from 0 to 320 inch/sec within a 31 microsecond time period.

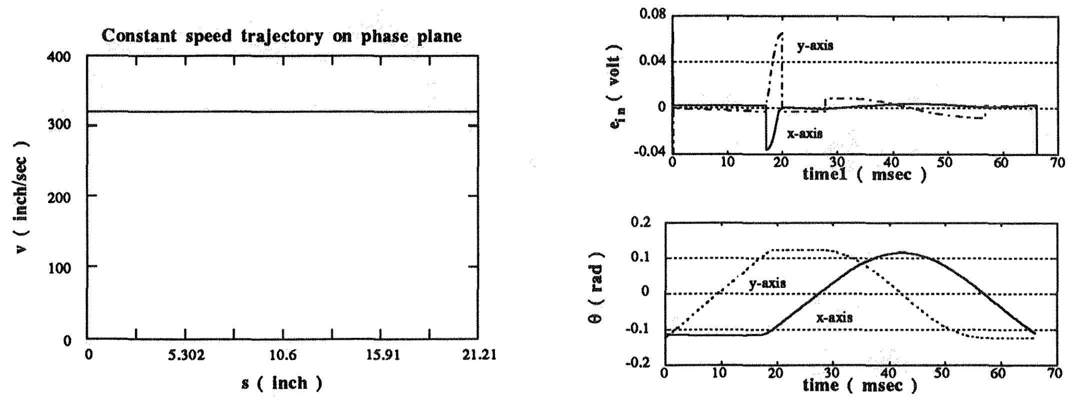

fig.10 The trajectory with 320 inch/sec tracking speed limit

IV. Feedback Control Design and Simulation

A model error exists since the control trajectory is solved with the simplified model. An input bias exists due to small current leakage from the power amplifier and an offset between mechanical neutral position and sensor neutral position. Therefore, a feedback control design is necessary to guarantee the tracking accuracy. Due to the difficulty in determining the weighting matrix in a LQG/LTR control method and the resulting high order compensator, a PID controller is chosen for feedback control design. The frequency response plots final closed loop transfer functions $T(s) = \Theta o(s)/\Theta i(s)$ which show 1.8K Hz bandwidth in x-axis, 1.8K Hz bandwidth in y-axis and $S(s) = \Theta o(s)/D(s)$. Good low frequency disturbance rejection is demonstrated where D(s) is the Laplace transform of the disturbance d(t). Both are are shown in fig.11. Good stability robustness is achieved by the stability margin in this design. The step time responses of T(s) and S(s) are shown in fig.12.

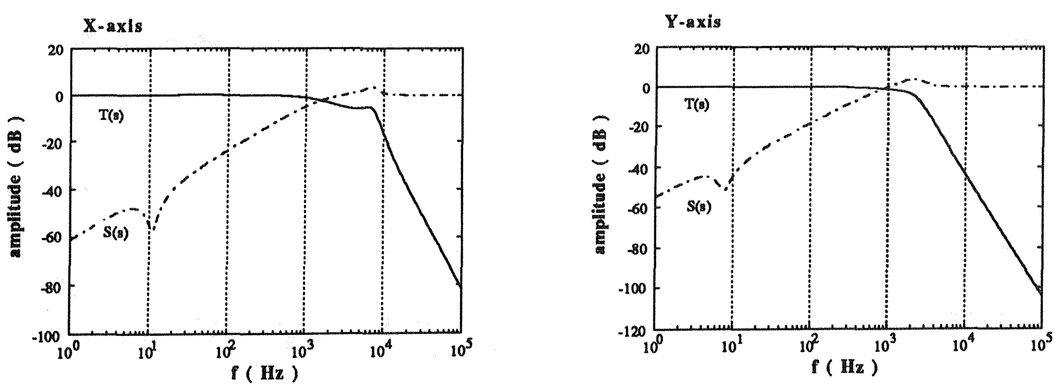

fig.11 The frequency response of the closed loop transfer function

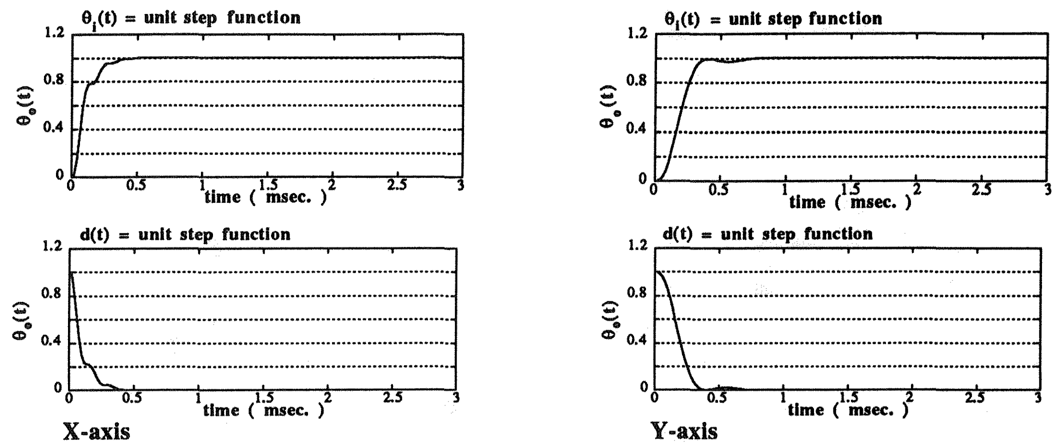

fig.12 The step time response of the closed loop transfer function

The digital control scheme with the feedback design is used in a simulation shown in fig.13. There are two ways to implement the control system with our results of open loop control trajectory planning and the feedback compensator design. One uses a position reference trajectory $\theta i(t)$ only, and the other uses both position reference trajectory $\theta i(t)$ and the designed control trajectory $e_{in}(t)$.

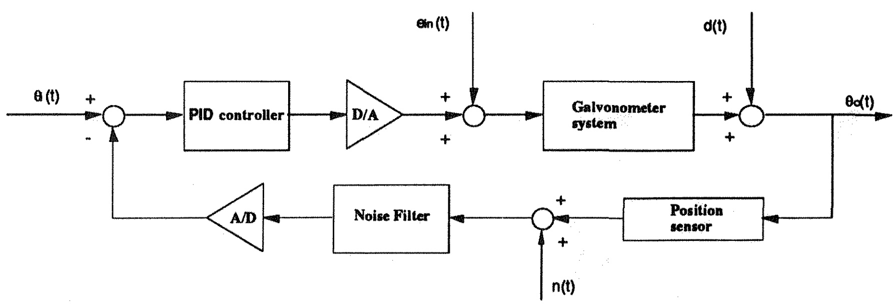

fig.13 The block diagram of control system

The simulation results of both implementations are shown in fig.14. There are three parameters defined to evaluate the performance of control design :

(1) the upper bound of position error on working surface :

$supError = max([(X_i - Xref_i)^2 + (Y_i - Yref_i)^2]^{0.5})$,

where (X_i, Y_i) is the actual position, $(Xref_i, Yref_i)$ is the reference position, i is index

(2) the root mean square (RMS) value of position error on working surface :

$rmsError = RMS([(X_i - Xref_i)^2 + (Y_i - Yref_i)^2]^{0.5})$

(3) the root mean square (RMS) value of control input e_{in} :

3.3 volts is the input limit in order to protect the galvonometer from overheating. Note the output of power amplifier is not saturated until the control input reaches 15 volts, rmsEin = RMS (e_{in}).

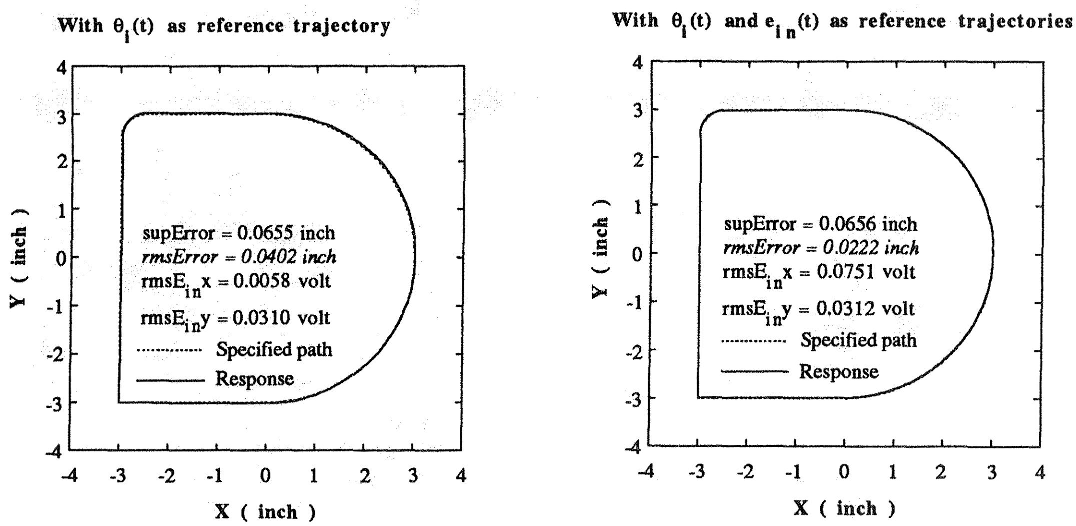

fig.14 The simulation results for both implementations

From fig.14 we see that the implementation with both position reference trajectory $\theta_i(t)$ and designed control trajectory $e_{in}(t)$ tracks the contour path better than the one with just $\theta_i(t)$ with the cost of computer storage for one extra trajectory per axis.

V. Conclusions

Based upon a well-identified galvonometer model in section II, a time-efficient laser tracking control system is designed for SFF applications. The optimal control trajectory is obtained as a reference. Due to the limits of available laser power, a lower tracking speed is required. A 320 inch/sec. tracking speed control trajectory is obtained. Both $\theta_i(t)$ and $e_{in}(t)$ are used in the control implementation scheme to improve the tracking accuracy. The conventional PID control design is used to obtain the simplest compensator with low computation load, good stability robustness, and good low frequency disturbance rejection. A designed trajectory of tracking speed v(t) is used as a reference for laser power on-line control without feedback to meet the requirement of uniform solidification based on an experimental model of solidification and the characteristics of an acousto-optic modulator which has at least 0.7M Hz bandwidth.

In further work, we propose to find the maximum allowable tracking speed at which a closed-loop galvonometer system may track a specified path with the required accuracy. The control design will be implemented by using a 386-base computer.

Reference

[1] Tomizuka, M., Dornfeld, D., Bian, X.-Q., and Cal, H.-G., " Experimental Evaluation of the Preview Servo Scheme for a Two-Axis Positioning System ", Journal of Dynamic Systems, Measurement, and Control, Transactions of the ASME, Vol. 106, March 1984, p.1-5.

[2] Doraiswami, R. and Gulliver, A., " A Control Strategy for Computer Numerical Control Machine Exhibiting Precision and Rapidity ", Journal of Dynamic Systems, Measurement, and Control, Transactions of the ASME, Vol. 106, March 1984, p.56-62.

[3] Kulkarni, P. K. and Srinivasan, K., " Cross Coupled Compensators for Contouring Control on Multi-axial Machine Tools ", 13th. North American Manufacturing Research Conference Proceedings, University Of California at Berkeley, Berkeley, California, May 19-22 1985, p.558-566.

[4] Tsao, Tsu-Chin , and Tomizuka, M., " Adaptive Zero Phase Error Tracking Algorithm for Digital Control ", Journal of Dynamic Systems, Measurement, and Control, Transactions of the ASME, Vol. 109, December 1987, p.349-354.

[5] Butler, J., Haack, B. and Tomizuka, M., " Reference Generation for High Speed Coordinated Motion of a Two Axis System ", Symposium on Robotics, The Winter Annual Meeting of the ASME, Chicago, Illinois, November 27 - December 2, 1988, p.457-470.

[6] Bobrow, J.E., Dubowsky, S. and Gibson, J. S., " Time-Optimal Control of Robotic Manipulators along Specified Paths ", The international Journal of Robotics Research, Vol.4, No.3, Fall 1985, p.3-17.

[7] Shin, Kang G. and McKay, Neil D., " Minimum-Time Control of Robotic Manipulators with Geometric Path Constraints ", IEEE Transaction on Automatic Control, Vol.AC-30, No.6, June 1985, p.531-541.

[8] Wu, Y.-J. and Beaman, J. J., " Contour Following for Scanning Control in SFF Application : Control Trajectory Planning ", presented at the Solid Freeform Fabrication Symposium, Austin, Texas, August 6-8, 1990.

[9] Doebelin, Ernest O., " Measurement systems ", McGraw-Hill, 1975, Sec.12.4.

[10] Montagu, Jean I., " Galvanometer and Resonant low inertia scanners ", General scanning Inc., 1985.

[11] Cambridge Technology, Inc., " Instruction Manual : Series 6000, Mirror Positioning System ", Watertown, MA 02172, 1990.

[12] Amnon Yariv, " Optical Electronics ", 3rd edition, CBS College Publishing, New York, 1985, Ch.9 and Ch.12.

[13] Robert Goldstein, " Electro-Optic Devices in Review : The Linear Electro-Optic (Pockels) Effect Forms the Basis for a Family of Active Devices ", Lasers and Applications, April, 1986.

[14] Adrian Korpel, " Acousto-Optics ", Marcel Dekker, Inc., New York, 1988, Sec.6.4.

[15] J. Sapriel, " Acousto-Optics ", John Wiley and Sons Ltd., New York, 1979, Sec.7.2, p.77.

[16] Robert Adler, " Interaction between light and sound ", IEEE Spectrum, May, 1967, p.42-54.

[17] John Lekavich, " Basics of Acousto-Optic Devices : Acousto-Optic Beam Modulators and Deflectors Control Laserbeam in Many Applications ", Lasers and Applications, April, 1986.

[18] IntraAction Corp., " Instruction Manual : AGM-406B Infrared Acousto-optic Modulator and GE-4030 Light Modulator Driver ", Bellwood, Ill 60104, 1990.